

# We are IntechOpen, the world's leading publisher of Open Access books Built by scientists, for scientists

6,900

Open access books available

186,000

International authors and editors

200M

Downloads

Our authors are among the

154

Countries delivered to

TOP 1%

most cited scientists

12.2%

Contributors from top 500 universities



WEB OF SCIENCE™

Selection of our books indexed in the Book Citation Index  
in Web of Science™ Core Collection (BKCI)

Interested in publishing with us?  
Contact [book.department@intechopen.com](mailto:book.department@intechopen.com)

Numbers displayed above are based on latest data collected.  
For more information visit [www.intechopen.com](http://www.intechopen.com)



# Multimodal Optical Imaging by Microendoscope

*Lin Huang and Zhen Qiu*

## Abstract

In the past decades, optical imaging field has been developing rapidly. Noninvasive imaging enabled by microendoscopes has become a promising tool for early cancer detection and imaging-guided surgery. In this chapter, we will mainly introduce most advances in the miniaturized microendoscope development, including photoacoustic, confocal fluorescence, multiphoton fluorescence, second-harmonic generation (SHG) label-free imaging, wide-field fluorescence, surface-enhanced Raman scattering (SERS) nanoparticle-based Raman spectroscopy. Enabled by the frontier micro-machining techniques, micro-opto-electromechanical system (MOEMS)-based novel microendoscopes with various imaging modalities have been prototyped and further translated into clinics. The working principle of representative microendoscopes and optical imaging modalities will be introduced in detail.

**Keywords:** optical imaging, microendoscope, micromachining, micro-opto-electromechanical systems (MOEMS), confocal, multiphoton, wide-field, photoacoustic, Raman, surface-enhanced Raman scattering (SERS)

## 1. Introduction

Optical imaging is a key part of molecular imaging which allows the in vivo characterization and measurement of biological process at the cellular and molecular level [1–3]. It uses the interaction between light and tissue to probe tissue morphology and functions. Compared to other molecular imaging techniques, such as magnetic resonance imaging (MRI) [4], computed tomography (CT) [5], ultrasound (US) [6], single-photon emission computed tomography (SPECT) [7], and positron-emission tomography (PET) [8], optical imaging builds an interdisciplinary approach to noninvasively probe disease-specific morphology and functions with high resolution. Biochemically specific contrast from light absorption, scattering, and fluorescence are widely used in optical imaging approaches, providing precise information from the tissue morphology, anatomy, and physiology. Optical imaging has been applied in a variety of biological research and is very useful in the early-stage diagnosis of diseases and monitoring the treatment outcomes [9, 10].

Optical imaging has been undergoing explosive growth over the past few decades since it is not limited to specific image-capture methods but includes various modalities, such as confocal fluorescence [11], wide-field fluorescence [12], multiphoton fluorescence and SHG imaging [13–15], photoacoustic tomography (PAT) [16], and SERS nanoparticle-based Raman spectroscopy [17–19] which are the major techniques optimized for different target visualization. The summary and comparisons are listed in **Table 1**. Wide-field, confocal, SERS-based Raman

	Contrast mechanism	Contrast agent	Wavelength	FOV	Resolution
<b>Confocal microendoscope [20]</b>	Reflectance and fluorescence	Fluorescein and acriflavine	488 nm	500 × 500 μm	Lateral: 0.7 mm Axial: 7 mm
<b>Wide-field fluorescence microendoscope [21]</b>	Fluorescence	MMPsense 645	424, 488, and 642 nm	70–100 degrees (air)	12 μm
<b>Multiphoton fluorescence and SHG microendoscope [22]</b>	Fluorescence and SHG	Label-free	750 nm	120 × 120 μm	Lateral: 833 nm Axial: 6.11 μm
<b>Photoacoustic microendoscope [23]</b>	Absorption	Label-free	584 nm	7 × 7 mm	Lateral: 80 μm Axial: 55 μm
<b>SERS based Raman microendoscope [24]</b>	Raman scattering	SERS nanoparticles	785 nm	5 cm in 360 degree	N/A

**Table 1.**

*A description and summary of various optical imaging modalities for in vivo endomicroscopy.*

imaging needs staining by applying contrast agent. Multiphoton and photoacoustic techniques, on the contrary, are capable of label-free imaging. Confocal imaging and multiphoton imaging enable submicron ( $<1 \mu\text{m}$ ) resolution and field of view (FOV) of  $500 \times 500 \mu\text{m}$ , while photoacoustic imaging has  $\sim 80 \mu\text{m}$  resolution and FOV of  $7 \times 7 \text{ mm}$ . Generally, there is a trade-off between FOV and resolution in optical imaging methods. To sum up, optical imaging techniques are noninvasive, offer a very high resolution at the cellular level, and provide contrast with biochemical specificity from light absorption, scattering, and fluorescence, with conventional microscopy techniques. However, the list of biological processes that can be investigated by these techniques is limited due to the large benchtop microscopes.

To fully translate the powerful optical imaging techniques into the in vivo clinical usage, miniaturization of the microscopes is essential. Enabled by the frontier micromachining techniques, micro-opto-electromechanical system (MOEMS)-based novel microendoscopes with various imaging modalities have been prototyped and further translated into clinics [25]. Consequently, multimodal imaging enabled by microendoscopes has become a promising tool for clinical applications in vivo, such as early cancer detection and imaging-guided surgery [26]. The amount of microendoscopes with different optical imaging techniques can be puzzling to anyone new to the field. In this chapter, the working principle of representative microendoscopes and optical imaging modalities will be introduced in detail.

## 2. Confocal imaging

Confocal imaging allows high-contrast imaging of a small spot within an optically transparent or translucent tissue by blocking most of the out-of-focus light through a pinhole to a detector [11]. The illumination point source and the detection pinhole are in optically conjugate focal planes and thus named as “confocal.” Compared to conventional optical microscopy, it provides better spatial resolution, controllable depth of field, and better image quality; and it is capable to collect optical sections of thick specimens. The contrasts provided by confocal imaging are generally reflectance [27] or fluorescence [28]. Promoted by the advances in fluorescence labeling, confocal microscopy has the capability of selectively imaging specific proteins at distinct cellular location [29]. However, the large microscope platform limits the application of confocal imaging within the laboratory.

Recently, a novel confocal microendoscope based on a single-mode fiber (SMF) acting as both the illumination point source and the detection pinhole was proposed by Kiesslich et al. [20]. Their laser colonoscope was integrated in the distal tip of a conventional videoendoscope, enabling endomicroscopically guided biopsies, shown in **Figure 1** [20]. The distal tip contained an air and water-jet nozzle, two light guides, an auxiliary water-jet channel (used for topical application of the contrast agent), and a 2.8-mm working channel. The diameters of the distal tip and the insertion tube were 13.4 and 12.8 mm, respectively. During laser endoscopy, a single-line laser delivered an excitation wavelength of 488 nm, and the maximum laser power output was  $\leq 1$  mW at the surface of the tissue. Confocal image data were collected at a scan rate of 0.8 frames per second (1024 by 512 pixels) or 1.6 frames per second (1024 by 1024 pixels). The optical slice thickness was 7 mm with a lateral resolution of 0.7 mm. The field of view was 500 by 500 mm. The range of the Z axis was 0–250 mm below the surface layer.

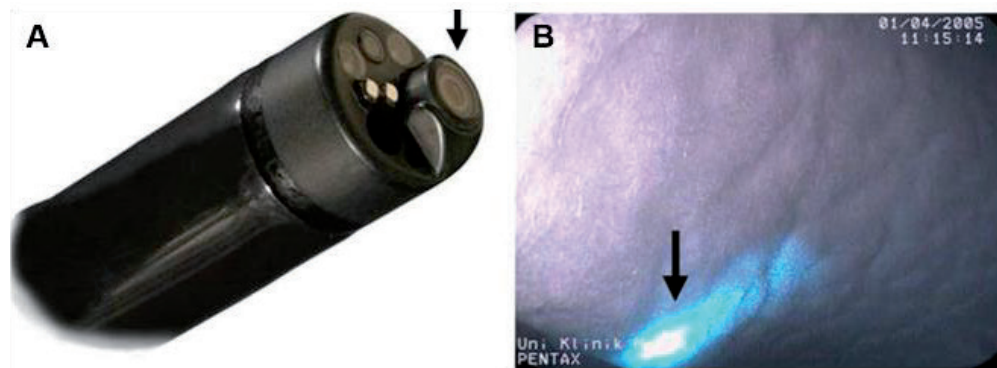


**Figure 1.**  
(A) Confocal laser colonoscope. (B) The blue laser light is clearly visible in the endoscopic view. Used with permission.

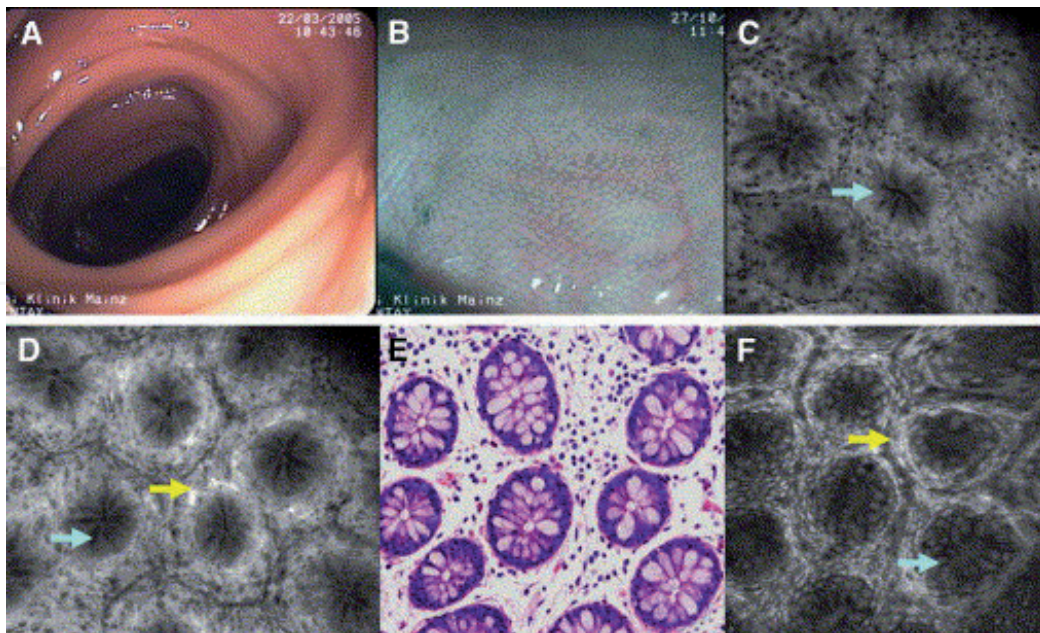


**Figure 2.**  
Upper row: optical possibilities of confocal endomicroscopy. (A) Normal endoscopic view. (B) High-resolution or magnifying endoscopy image. (C) Confocal endomicroscopy image. Lower row: normal crypt architecture. (D) Confocal endomicroscopy with fluorescein intravenously given. (E) Conventional histology in horizontal sectioning of normal crypt architecture. (F) Confocal endomicroscopy after topical application of acriflavine. Used with permission.

To achieve high-resolution confocal imaging, exogenous fluorescence agents were applied. In human studies, fluorescein (10%; colon, esophagus, stomach) and topically applied acriflavine (0.2%; stomach, colon) were used most often. By using these exogenous fluorescence techniques, confocal images were acquired simultaneously with endoscopic images, making it possible to identify typical histological structures in the human gastrointestinal tract, shown in **Figure 2** [20]. This confocal microendoscope was further applied to detect cellular and vascular changes and distinguish different types of epithelial cell [30].

### 3. Wide-field fluorescence imaging

Wide-field fluorescence imaging allows rapid visualization of large surface areas in hollow organs, leading to disease localization and optical biopsy guidance [12]. With the advances in miniaturization of video charge-coupled device (CCD) chip, wide-field fluorescence imaging by microendoscope is involving rapidly [31]. By scanning a SMF in a spiral pattern through a tubular piezoelectric actuator, a scanning fiber endoscopy (SFE) was proposed to create an image with a large field of view (FOV) and high resolution [21, 32]. The SFE consisted of an ultrathin, highly flexible catheter that scans blue, green, and red laser beams (wavelengths are 424, 488, and 642 nm) in a spiral pattern on the tissue surface (**Figure 3A** and **B**) and collected reflectance and fluorescence through a ring of optical fibers (**Figure 3C–E**) [21]. The distal tip had an outer diameter of 3.17 mm and had a 11.5 cm rigid end. By combining reflectance

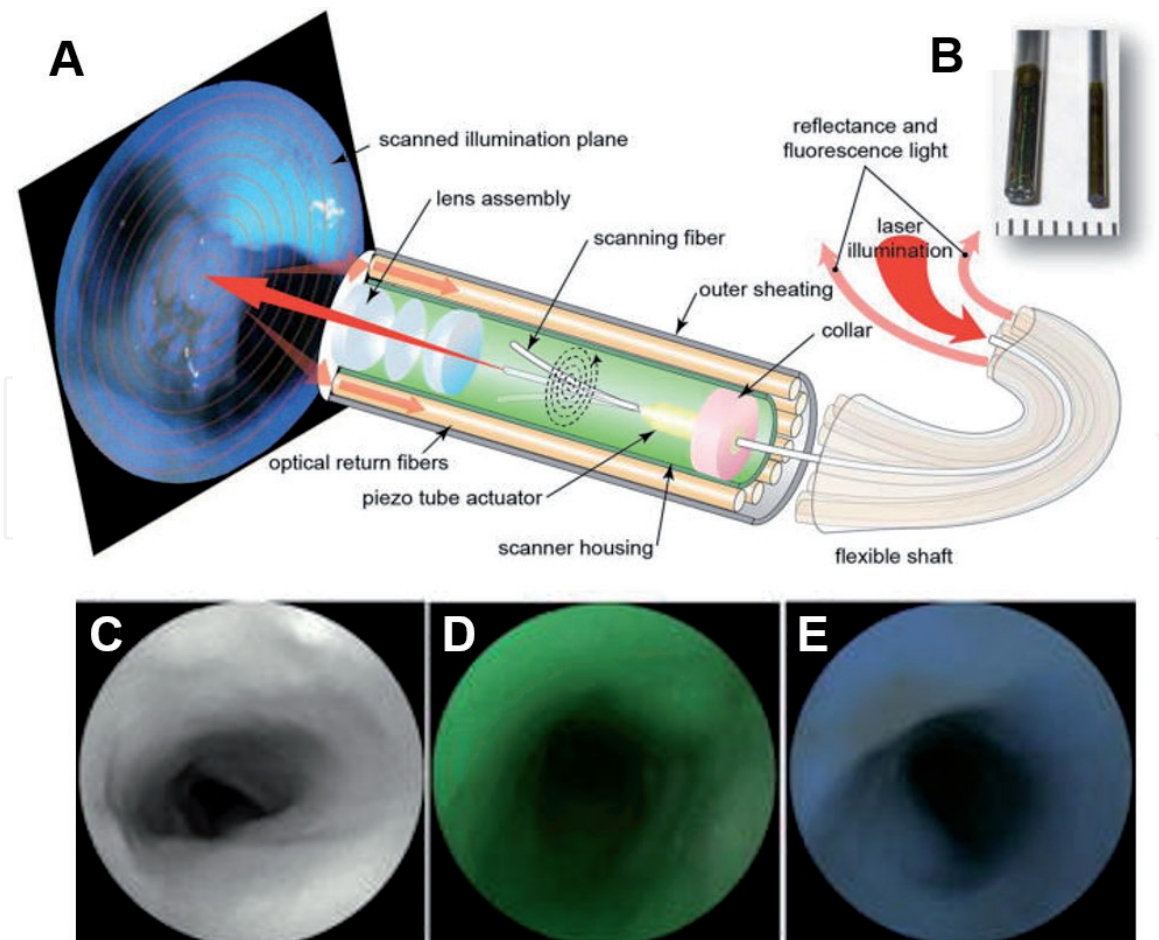


**Figure 3.** The schematic of SFE (A) and a photo of the distal end (B). (C) White light endoscopic system image under reflectance and laser mode. (D) Reflectance and laser-induced green fluorescence. (E) Reflectance and laser-induced blue fluorescence. Used with permission.

and laser-induced fluorescence of intrinsic fluorescent constituents in tissue, the SFE enabled video rate (30 frames/s) imaging to overcome motion artifacts in vivo.

This technique was initially proposed to detect fluorescence to visualize overexpressed molecular targets [33]. Recently, it was demonstrated as a multimodal laser-based angioscopy which is potentially a powerful platform for research, diagnosis, prognosis, and image-guided local therapy in atherosclerosis and cardiovascular disease [21]. The small size of the SFE allowed for collecting high-resolution images from the esophagus, stomach, and colon in the mouse models to perform in-depth imaging for study of molecular mechanisms of disease [34, 35]. The compact probe design based on spiral scanning of fiber instrument enabled a miniature package compatible with standard medical endoscopes.

#### 4. Multiphoton fluorescence and SHG

Multiphoton fluorescence and second-harmonic generation (SHG) are nonlinear imaging techniques for noninvasive, high-resolution, real-time diagnostics of tissues at subcellular resolution. They are based on exciting and detecting nonlinear optical signals from biological tissues [13–15]. Femtosecond laser pulses are used to excite nonlinear signals such as two-photon-excited fluorescence (TPEF) and SHG from tissue [2]. Consequently, depth-resolved imaging is enabled because the excitation of nonlinear signals happens only within the focal volume of the laser beam. It is a functional imaging technique in which the contrasts from nicotinamide adenine dinucleotide hydrogen (NADH), flavin adenine dinucleotide (FAD), elastin, and collagen are biochemically specific. Therefore, they allow label-free imaging without any exogenous contrast agent. Currently, multiphoton fluorescence and SHG microscopy have mainly been carried out on a microscope stage on the laboratory bench [13–15]. For in vivo imaging and clinical applications, a fiber-optic-based microendoscope is needed where light can be delivered through a flexible fiber and images can be acquired using a miniature probe [36–38].

The Chris Xu group at Cornell University used piezoelectric actuators and a miniaturized high NA gradient-index (GRIN) lens to form a compact and flexible two-photon fluorescence (TPF)/SHG endoscope, which had an outside diameter of 3 mm and a rigid length of 4 cm, shown in **Figure 4** [37]. They achieved imaging at approximately a speed of 4.1 frames/s. GRIN lens has a small diameter and cylindrical geometry. However, it suffers from severe chromatic aberration and causes a considerable focal shift between the excitation wavelength (NIR) and the TPEF and SHG signal wavelength (visible).

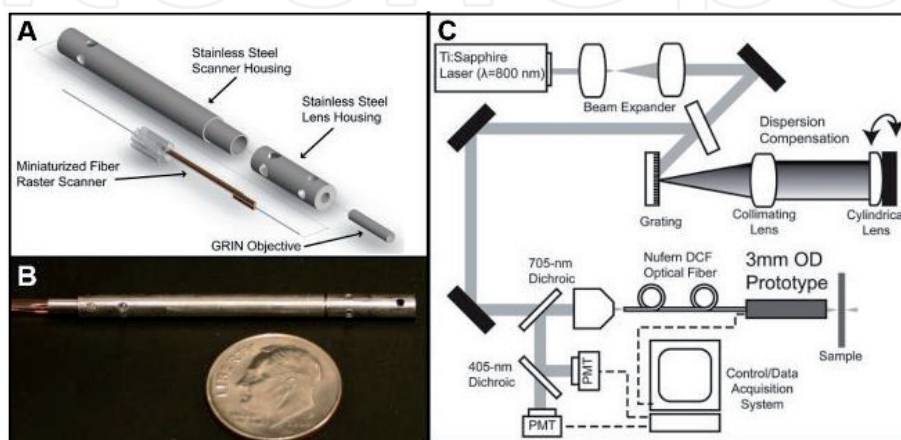


**Figure 4.** System components and setup. (A) Mechanical assembly of the microendoscope. (B) Photograph of the prototype. (C) Imaging setup. Used with permission.

Ex vivo images of mouse tissue was acquired as shown in **Figure 5** [37]. In tissue, SHG contrast mainly comes from collagen, and thus it is especially useful for imaging cartilage, bone, tendon, the skin, and cornea where collagen is the most abundant extracellular matrix protein in the tissues [39]. TPEF signal derives from intrinsic autofluorescence sources, such as elastin, NADH, and flavins. The intrinsic TPEF signal can be observed from cells, collagen, and elastin fibers.

The rigid probe based on a GRIN lens is more desirable in laparoscopic applications or in interfacing with a biopsy probe. Currently, the Xingde Li group developed a handheld rigid probe with multiphoton fluorescence and SHG techniques for optical biopsy (**Figure 6A–C**) [22]. In the rigid probe, two functional parts are a handheld compact scanning box (3D) and a compound GRIN objective which was 15 cm long with an outer diameter of 1.75 mm. The probe could fit within a 14-gauge biopsy needle. The scanning box included a MEMS mirror for

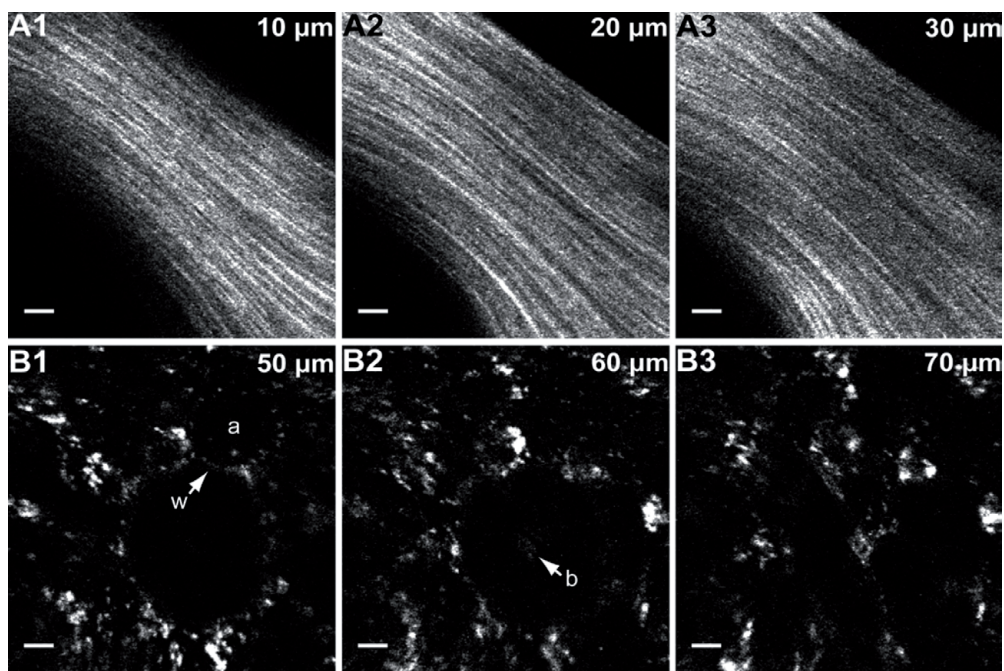


**Figure 5.** TPEF/SHG images of ex vivo mouse tissue. (A) Unaveraged SHG images of mouse tail tendon at 10, 20, and 30  $\mu\text{m}$  from the surface. (B) Unaveraged intrinsic fluorescence images of mouse lung at 50, 60, and 70  $\mu\text{m}$  from the tissue surface. Used with permission.

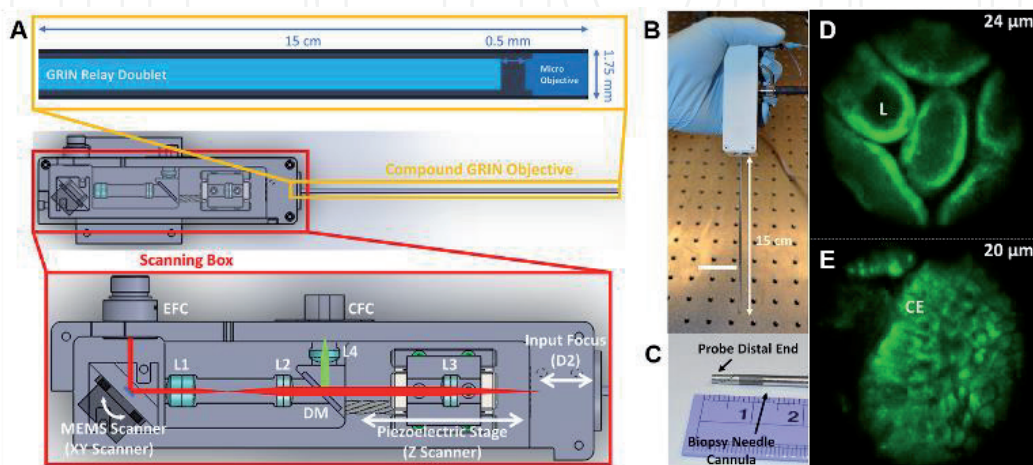


**Figure 6.** Handheld rigid probe and TPEF images. (A) Handheld probe design schematic. (B) Photo of the handheld rigid probe. (C) Photo of the rigid probe inside a 14-gauge biopsy needle. In vivo TPEF images of the mouse kidney cortex (D) and mouse small intestinal mucosa (E). Scale bar, 20  $\mu\text{m}$ . Used with permission.

two-dimensional (2D) raster beam scanning up to 10 frames/s and a piezoelectric stage for axial scanning. A SMF was used for delivery of femtosecond pulses, and a multimode fiber (MMF) with a large core diameter was used at the proximal end of the rigid probe to deliver the signal to a detector. In vivo images of the mouse kidney cortex and intestinal mucosa were acquired as shown in **Figure 6D** and **E**, with an imaging depth which was up to 24  $\mu\text{m}$  [22].

## 5. Photoacoustic tomography

The drawback of pure optical imaging (both linear and nonlinear) in biological tissue is that the strong optical scattering causes shallow imaging depth ( $\sim 1\text{--}2$  mm). Photoacoustic tomography (PAT) is a relatively new technique that overcomes the limitations of existing pure optical imaging by detecting optical absorption contrast via the photoacoustic (PA) effect [16]. In PAT, a laser excites photoacoustic waves generated by rapid thermoelastic expansion through optical absorption of short laser pulse (PA effect), and ultrasound transducers detect the photoacoustic waves [40]. The major advantage of PAT is that it can image biological tissues in vivo with high spatial resolution for up to a few centimeters of penetration depth. Additionally, PAT allows label-free imaging with endogenous contrast. Thus, the PAT technique has been evolving rapidly with applications in various biological processes over the past decade.

A PAT microendoscope (**Figure 7A–D**) with simultaneous photoacoustic and ultrasonic imaging was implemented by the Lihong Wang group [41]. A rotating mirror acting as a scanner reflected the ultrasonic waves and laser pulses, and it was statically mounted with the associated illumination and ultrasonic pulse-generation detection units. The reflected ultrasonic and photoacoustic waves were detected and converted into electric signals via the ultrasonic transducer to a computer. By inserting the side-scanning 3.8-mm-diameter probe prototype into the esophagus, surrounding organs, such as the lung and trachea, were observed in both the photoacoustic and ultrasonic images (**Figure 7F–K**) [41]. However, only photoacoustic images showed their adjacent vasculatures. These experimental results demonstrated the deep imaging ability of the dual-mode microendoscope and the

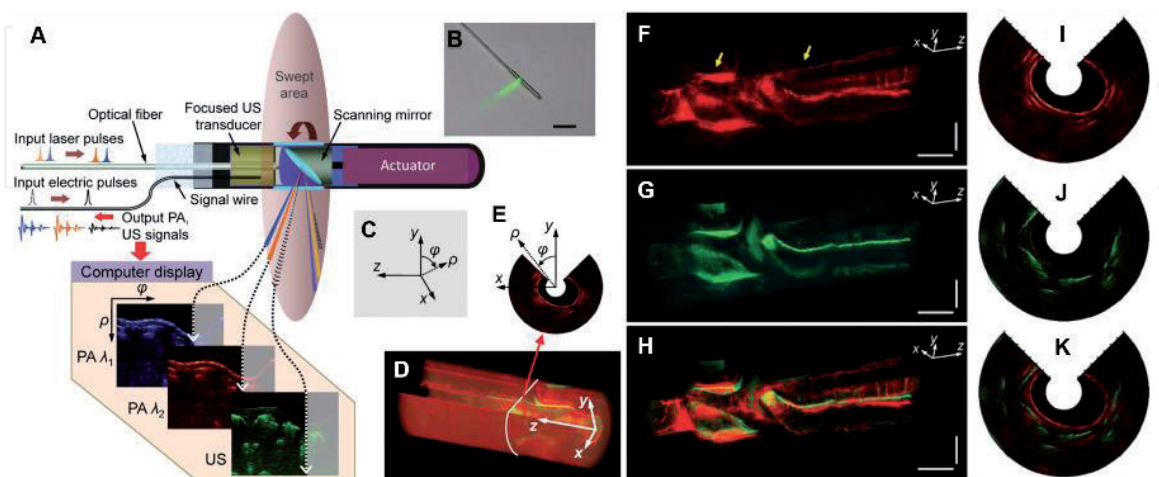


**Figure 7.**

*Illustration of simultaneous, multiwavelength PA and ultrasonic endoscopy. (A) The endoscope design. (B) A photo shows the side-scanning 3.8-mm-diameter probe prototype. Scale bar, 2 cm. (C) Definition of Cartesian and cylindrical coordinate systems. (D) A volumetric image. (E) A representative cross section of  $d$  along the  $x$ - $y$  plane. (F) Three-dimensionally rendered PA structural image. (G) Co-registered US structural image for the same volume of F. (H) An overlaid image of F and G. The horizontal and vertical scale bars are 2 cm and 5 mm, respectively. (I) A representative PA  $x$ - $y$  cross-sectional image (18 mm diameter) near the lung. (J) Corresponding US cross-sectional image of I. (K) A combined image of I and J. Used with permission.*

complementary contrast production. To further explore this microendoscope's potential, *in vivo* PA imaging of two rabbit esophagi was conducted, where high-resolution, three-dimensional microvasculature distribution in the esophagi walls and neighboring mediastinal regions was imaged [23].

## 6. SERS nanoparticle-based Raman spectroscopy

Surface-enhanced Raman scattering (SERS) is a plasmonic effect resulting enhanced Raman signals from molecules which have been attached to nanometer-sized metallic structures [17–19]. SERS nanoparticle-based Raman spectroscopy is a spectrally molecular imaging technique allowing for ultrahigh sensitivity and the unique ability to multiplex readouts from a variety of molecular targets using a single wavelength of excitation [42]. Based on SERS nanoparticles (~120 nm in diameter) in small animals, a Raman imaging instrument that enabled rapid, high-spatial resolution, spectroscopic imaging over a wide field of view (>6 cm<sup>2</sup>) was proposed [43, 44]. In the Raman imaging system, the gold-based nanoparticles (S420, S421, S440, and S470 as shown in **Figure 8**) can dramatically increase the Raman scattered light emitted by small molecules adsorbed onto the surface [45, 46]. The advantage of multiplexing is that it simultaneously detects multiple biomarkers if each type of nanoparticles binds to a different protein target. Consequently, verity types of conjugated SERS nanoparticles with the tumor-targeting capabilities in preclinical animal models have been investigated [47–50].

To translate of this imaging approach to the clinic, a small, flexible, fiber-optic-based Raman imaging microendoscope, designed for GI tract (such as within the colon or esophagus) imaging, were proposed (**Figure 9A and D**) [24]. It utilized circumferential scanning to map of the signal from SERS nanoparticles located on a luminal surface (**Figure 9B and C**). The scan mirror was located between the collimating lens and the tissue and is angled at 50° to provide a radial projection of the illumination beam. As it rotated about its axis, the illumination beam swept around the device resulting in a 360° circumferential scan of the tissue. *In vivo* human study was conducted by using the imaging system packaged in the endoscopy suite, and the three-dimensional topography of the colon could is recreated (**Figure 9E–H**). These results provided an anatomic reference image on which the molecular data can be mapped. One advantage of SERS nanoparticle-based Raman microendoscope is that its noncontact feature allows the user to scan large, topologically complex surfaces much faster than devices requiring tissue contact [24]. Additionally, the enhanced Raman effect can occur within the entire plasmon

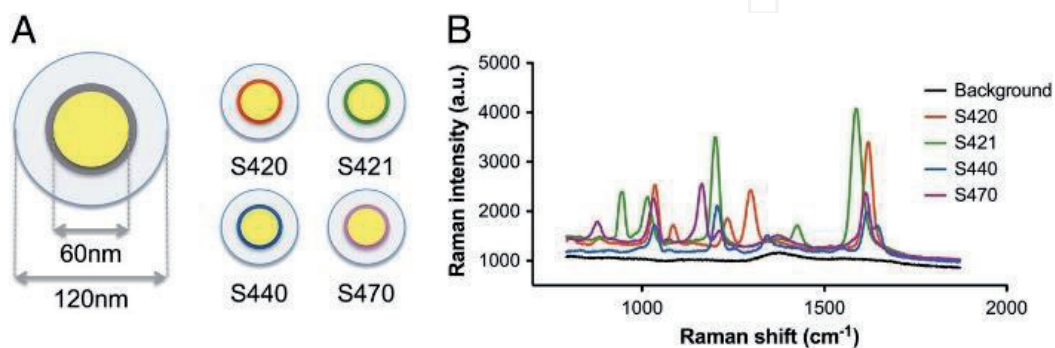


**Figure 8.** Schematic representation of SERS nanoparticles and their Raman spectra. (A) Gold nanoparticles are covered with a layer of Raman active material and then a silica coating. (B) The spectral fingerprint of different Raman active materials with laser excitation at 785 nm. The background spectrum is acquired in the same experimental arrangement without nanoparticles. Used with permission.

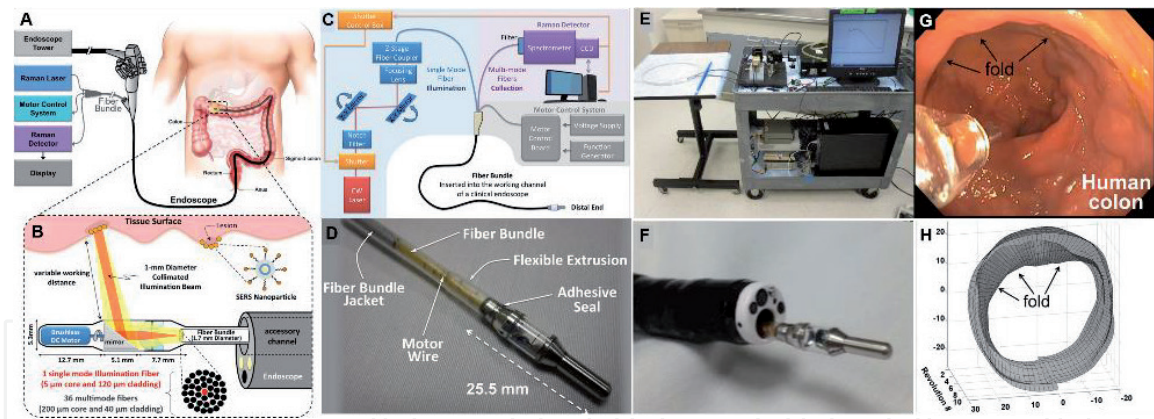


**Figure 9.** Schematic of Raman imaging system and clinical application. (A) The device can be inserted through the colon. (B) Expanded schematic of the distal end. (C) System overview. (D) Close-up photograph of the distal end. (E) The imaging system in the endoscopy suite. (F) The device inserted and exiting from the distal end of a clinical endoscope. (G) The device being used in first human clinical study (C). (H) A three-dimensional reconstruction of the topography of the colon (D). Used with permission.

resonance spectrum of the nanoparticles, while fluorescein only happens at comparably narrow absorption peaks which vary with each fluorophore. Moreover, SERS nanoparticles do not suffer from photo bleaching, which is a limitation of fluorophore-based endoscopy.

## 7. Conclusions

Today, multimodal optical imaging by microendoscope has been evolving rapidly, leading to a diversity of exciting biological discoveries and clinical applications. It is an invaluable diagnostic approach allowing minimally invasive, real-time, subcellular access to tissues deep within the body, such as the oropharynx, esophagus, lung, stomach, colon, and rectum. Advanced endomicroscopes have been enabled by the advances in light sources, micro-optics, fiber optics, miniature scanner. Additionally, innovative target-specific nanoparticles could probe early disease detection before morphology changes occur. The miniature microendoscope system potentially allows for imaging beyond gross anatomical structures to appreciate biological function. In the future, directions toward more informative ways will include finer spatial resolution, sharper contrast, higher imaging speed, deeper penetration, and greater detection sensitivity. Further efforts lie in preclinical trial and clinical trail through the cross-disciplinary collaborations.

## Conflict of interest

The authors have no financial interests or potential conflict of interest to disclose concerning this work.

IntechOpen

IntechOpen

### **Author details**

Lin Huang and Zhen Qiu\*

Department of Biomedical Engineering, Institute for Quantitative Health Science and Engineering, Michigan State University, East Lansing, USA

\*Address all correspondence to: [qiuzhen@egr.msu.edu](mailto:qiuzhen@egr.msu.edu)

### **IntechOpen**

---

© 2019 The Author(s). Licensee IntechOpen. This chapter is distributed under the terms of the Creative Commons Attribution License (<http://creativecommons.org/licenses/by/3.0>), which permits unrestricted use, distribution, and reproduction in any medium, provided the original work is properly cited. 

## References

- [1] Weissleder R, Mahmood U. Molecular imaging. *Radiology*. 2001;**219**:316-333
- [2] Weissleder R. Molecular imaging in cancer. *Science*. 2006;**312**:1168-1171
- [3] Willmann JK, Van Bruggen N, Dinkelborg LM, Gambhir SS. Molecular imaging in drug development. *Nature Reviews Drug Discovery*. 2008;**7**:591
- [4] Ogawa S, Lee T-M, Kay AR, Tank DW. Brain magnetic resonance imaging with contrast dependent on blood oxygenation. *Proceedings of the National Academy of Sciences*. 1990;**87**:9868-9872
- [5] Agatston AS, Janowitz WR, Hildner FJ, Zusmer NR, Viamonte M, Detrano R. Quantification of coronary artery calcium using ultrafast computed tomography. *Journal of the American College of Cardiology*. 1990;**15**:827-832
- [6] Aaslid R, Markwalder T-M, Nornes H. Noninvasive transcranial Doppler ultrasound recording of flow velocity in basal cerebral arteries. *Journal of Neurosurgery*. 1982;**57**:769-774
- [7] Hachamovitch R, Berman DS, Shaw LJ, Kiat H, Cohen I, Cabico JA, et al. Incremental prognostic value of myocardial perfusion single photon emission computed tomography for the prediction of cardiac death: Differential stratification for risk of cardiac death and myocardial infarction. *Circulation*. 1998;**97**:535-543
- [8] Gambhir SS. Molecular imaging of cancer with positron emission tomography. *Nature Reviews Cancer*. 2002;**2**:683
- [9] Yang M, Baranov E, Jiang P, Sun F-X, Li X-M, Li L, et al. Whole-body optical imaging of green fluorescent protein-expressing tumors and metastases. *Proceedings of the National Academy of Sciences*. 2000;**97**:1206-1211
- [10] Ntziachristos V. Going deeper than microscopy: The optical imaging frontier in biology. *Nature Methods*. 2010;**7**:603
- [11] Pawley J. *Handbook of Biological Confocal Microscopy*. New York, USA: Springer Science & Business Media; 2010
- [12] Ganten D, Ruckpaul K, Birchmeier W, Epplen JT, Genser K, Gossen M, et al, editors. *Wide-field fluorescence Microscopy*. In: *Encyclopedic Reference of Genomics and Proteomics in Molecular Medicine*. Berlin, Heidelberg: Springer; 2006. p. 1998
- [13] Denk W, Strickler JH, Webb WW. Two-photon laser scanning fluorescence microscopy. *Science*. 1990;**248**:73-76
- [14] Zipfel WR, Williams RM, Webb WW. Nonlinear magic: Multiphoton microscopy in the biosciences. *Nature Biotechnology*. 2003;**21**:1369-1377
- [15] Campagnola PJ, Loew LM. Second-harmonic imaging microscopy for visualizing biomolecular arrays in cells, tissues and organisms. *Nature Biotechnology*. 2003;**21**:1356-1360
- [16] Wang LV, Hu S. Photoacoustic tomography: In vivo imaging from organelles to organs. *Science*. 2012;**335**:1458-1462
- [17] Kneipp K, Wang Y, Kneipp H, Perelman LT, Itzkan I, Dasari RR, et al. Single molecule detection using surface-enhanced Raman scattering (SERS). *Physical Review Letters*. 1997;**78**:1667
- [18] Kneipp K, Kneipp H, Itzkan I, Dasari RR, Feld MS. Surface-enhanced

- Raman scattering and biophysics. *Journal of Physics: Condensed Matter*. 2002;**14**:R597
- [19] Le Ru E, Blackie E, Meyer M, Etchegoin PG. Surface enhanced Raman scattering enhancement factors: A comprehensive study. *The Journal of Physical Chemistry C*. 2007;**111**:13794-13803
- [20] Kiesslich R, Goetz M, Vieth M, Galle PR, Neurath MF. Confocal laser endomicroscopy. *Gastrointestinal Endoscopy Clinics*. 2005;**15**:715-731
- [21] Savastano LE, Zhou Q, Smith A, Vega K, Murga-Zamalloa C, Gordon D, et al. Multimodal laser-based angioscopy for structural, chemical and biological imaging of atherosclerosis. *Nature Biomedical Engineering*. 2017;**1**:0023
- [22] Li A, Hall G, Chen D, Liang W, Ning B, Guan H, et al. A biopsy-needle compatible varifocal multiphoton rigid probe for depth-resolved optical biopsy. *Journal of Biophotonics*. 2019;**12**:e201800229
- [23] Yang JM, Favazza C, Yao J, Chen R, Zhou Q, Shung KK, et al. Three-dimensional photoacoustic endoscopic imaging of the rabbit esophagus. *PLoS One*. 2015;**10**:e0120269
- [24] Garai E, Sensarn S, Zavaleta CL, Loewke NO, Rogalla S, Mandella MJ, et al. A real-time clinical endoscopic system for intraluminal, multiplexed imaging of surface-enhanced Raman scattering nanoparticles. *PLoS One*. 2015;**10**:e0123185
- [25] Qiu Z, Wang TD. Engineering miniature imaging instruments. In: Cai W, editor. *Engineering in Translational Medicine*. London: Springer; 2014. pp. 835-852
- [26] Kiesslich R, Burg J, Vieth M, Gnaendiger J, Enders M, Delaney P, et al. Confocal laser endoscopy for diagnosing intraepithelial neoplasias and colorectal cancer in vivo. *Gastroenterology*. 2004;**127**:706-713
- [27] González S, Tannous Z. Real-time, in vivo confocal reflectance microscopy of basal cell carcinoma. *Journal of the American Academy of Dermatology*. 2002;**47**:869-874
- [28] Rajadhyaksha M, Grossman M, Esterowitz D, Webb RH, Anderson RR. In vivo confocal scanning laser microscopy of human skin: Melanin provides strong contrast. *Journal of Investigative Dermatology*. 1995;**104**:946-952
- [29] Polglase AL, McLaren WJ, Skinner SA, Kiesslich R, Neurath MF, Delaney PM. A fluorescence confocal endomicroscope for in vivo microscopy of the upper-and the lower-GI tract. *Gastrointestinal Endoscopy*. 2005;**62**:686-695
- [30] Kiesslich R, Gossner L, Goetz M, Dahlmann A, Vieth M, Stolte M, et al. In vivo histology of Barrett's esophagus and associated neoplasia by confocal laser endomicroscopy. *Clinical Gastroenterology and Hepatology*. 2006;**4**:979-987
- [31] Elahi SF, Wang TD. Future and advances in endoscopy. *Journal of Biophotonics*. 2011;**4**:471-481
- [32] Lee CM, Engelbrecht CJ, Soper TD, Helmchen F, Seibel EJ. Scanning fiber endoscopy with highly flexible, 1 mm catheterscopes for wide-field, full-color imaging. *Journal of Biophotonics*. 2010;**3**:385-407
- [33] Miller SJ, Joshi B, Wang TD-S, Lee CM, Seibel EJ, Gaustad A. Targeted detection of murine colonic dysplasia in vivo with flexible multispectral scanning fiber endoscopy. *Journal of Biomedical Optics*. 2012;**17**:021103
- [34] Miller SJ, Joshi BP, Feng Y, Gaustad A, Fearon ER, Wang TD.

In vivo fluorescence-based endoscopic detection of colon dysplasia in the mouse using a novel peptide probe. *PLoS One*. 2011;**6**:e17384

[35] Elahi SF, Miller SJ, Joshi B, Wang TD. Targeted imaging of colorectal dysplasia in living mice with fluorescence microendoscopy. *Biomedical Optics Express*. 2011;**2**:981-986

[36] Zhang Y, Akins ML, Murari K, Xi J, Li M-J, Luby-Phelps K, et al. A compact fiber-optic SHG scanning endomicroscope and its application to visualize cervical remodeling during pregnancy. *Proceedings of the National Academy of Sciences*. 2012;**109**:12878-12883

[37] Rivera DR, Brown CM, Ouzounov DG, Pavlova I, Kobat D, Webb WW, et al. Compact and flexible raster scanning multiphoton endoscope capable of imaging unstained tissue. *Proceedings of the National Academy of Sciences*. 2011;**108**(43):17598-17603

[38] Piyawattanametha W, Cocker ED, Burns LD, Barretto RP, Jung JC, Ra H, et al. In vivo brain imaging using a portable 2.9 g two-photon microscope based on a microelectromechanical systems scanning mirror. *Optics Letters*. 2009;**34**:2309-2311

[39] Zoumi A, Yeh A, Tromberg BJ. Imaging cells and extracellular matrix in vivo by using second-harmonic generation and two-photon excited fluorescence. *Proceedings of the National Academy of Sciences*. 2002;**99**:11014-11019

[40] Zhang HF, Maslov K, Stoica G, Wang LV. Functional photoacoustic microscopy for high-resolution and noninvasive in vivo imaging. *Nature Biotechnology*. 2006;**24**:848

[41] Yang J-M, Favazza C, Chen R, Yao J, Cai X, Maslov K, et al. Simultaneous

functional photoacoustic and ultrasonic endoscopy of internal organs in vivo. *Nature Medicine*. 2012;**18**:1297

[42] Palonpon AF, Ando J, Yamakoshi H, Dodo K, Sodeoka M, Kawata S, et al. Raman and SERS microscopy for molecular imaging of live cells. *Nature Protocols*. 2013;**8**:677

[43] Bohndiek SE, Wagadarikar A, Zavaleta CL, Van de Sompel D, Garai E, Jokerst JV, et al. A small animal Raman instrument for rapid, wide-area, spectroscopic imaging. *Proceedings of the National Academy of Sciences*. 2013;**110**:12408-12413

[44] Garai E, Sensarn S, Zavaleta CL, Van de Sompel D, Loewke NO, Mandella MJ, et al. High-sensitivity, real-time, ratiometric imaging of surface-enhanced Raman scattering nanoparticles with a clinically translatable Raman endoscope device. *Journal of Biomedical Optics*. 2013;**18**:096008

[45] Zavaleta CL, Smith BR, Walton I, Doering W, Davis G, Shojaei B, et al. Multiplexed imaging of surface enhanced Raman scattering nanotags in living mice using noninvasive Raman spectroscopy. *Proceedings of the National Academy of Sciences*. 2009;**106**:13511-13516

[46] Zavaleta CL, Garai E, Liu JT, Sensarn S, Mandella MJ, Van de Sompel D, et al. A Raman-based endoscopic strategy for multiplexed molecular imaging. *Proceedings of the National Academy of Sciences*. 2013;**110**:E2288-E2297

[47] Keren S, Zavaleta C, Cheng Z, de La Zerda A, Gheysens O, Gambhir S. Noninvasive molecular imaging of small living subjects using Raman spectroscopy. *Proceedings of the National Academy of Sciences*. 2008;**105**:5844-5849

[48] Zavaleta C, De La Zerda A, Liu Z, Keren S, Cheng Z, Schipper M, et al. Noninvasive Raman spectroscopy in living mice for evaluation of tumor targeting with carbon nanotubes. *Nano Letters*. 2008;**8**:2800-2805

[49] Qian X, Peng X-H, Ansari DO, Yin-Goen Q, Chen GZ, Shin DM, et al. In vivo tumor targeting and spectroscopic detection with surface-enhanced Raman nanoparticle tags. *Nature Biotechnology*. 2008;**26**:83

[50] Dinish U, Balasundaram G, Chang Y-T, Olivo M. Actively targeted in vivo multiplex detection of intrinsic cancer biomarkers using biocompatible SERS nanotags. *Scientific Reports*. 2014;**4**:4075

IntechOpen